

A Study on Multipole BLDC Sensorless Control Methods based on Integration of Non-excited Phase Back-EMF

¹Jin-Wook Park, ²Myeong-Hwan Hwang, ³Dong-Hyeon Kim, ⁴Hyun-Rok Cha, ⁵Sung-Jun Park, ^{*6}Seong-Mi Park

^{1,5}Dept. of Electrical Engineering, Chonnam National University, Gwangju 61186, Korea

^{2,3,4}Dept. of Automotive Components & Materials R&D Group, KITECH, Gwangju 61012, Korea

⁶Dept. of Lift Design, Korea Lift College, Geochang 50141, Korea

*Corresponding author E-mail: ¹hebojago@naver.com, ²han9215@kitech.re.kr, ³bjuuh2608@kitech.re.kr, ⁴hrcha@kitech.re.kr, ⁵sjpark1@jnu.ac.kr, ^{*6}seongmi@klc.ac.kr

Abstract

Background/Objectives: As multipolar electric motors have been widely used recently, studies on high-capacity multipole BLDC sensorless control methods have attracted attention.

Methods/Statistical analysis: There is a compelling need for stable sensorless control methods because high-capacity multipole BLDC motors by multipolarization has a high frequency of voltage applied by high-speed operation. Therefore, in this paper we proposed a new sensorless control method for counter electromotive force in the non-conducting periods on both sides of the conducting periods of BLDC motors driven in the 120° conduction mode. The proposed sensorless control method switches to integrate counter electromotive force in the non-conducting period and to control the values. In addition, this paper tested the validity of the proposed method for 4 kw-class 28-pole BLDC motors.

Findings: The proposed method made it possible to realize sensorless strongly resistant to noise by realizing sensorless based on integrating counter electromotive force. To control the ratio of the integrated values of counter electromotive force makes it possible to adjust switching periods and to realize various controls such as field-weakening control.

Improvements/Applications: It can be used in the case of multi-pole high-speed operation, It is expected that it will be widely used for drone BLDC motor and electric kickboard which is difficult to install position sensor.

Keywords: Sensorless control, BLDC motor driver, Multipole BLDC, PMSM motor driver, PMSM Sensorless control

1. Introduction

With the development of the electric motor industry, various capacity multipole BLDC motors have been actively produced. Due to the nature of multipole BLDC motors, they are driven at high speed to realize high-energy densification by reducing the weight of electric motors. The BLDC motors with encoders or hall effect sensors to be driven have a greater burden such as size densification and vibration in high speed operation than previous BLDC motors. Thus, in order to reduce this burden, there is a fast growing demand for sensorless control. In particular, the studies on stable sensorless control methods have attracted attention because of high-capacity multipole BLDC motors by multipolarization has a high frequency of voltage applied in high-speed operation[1-4].

Therefore, in this paper proposed a new sensorless control method for counter electromotive force in the non-conducting periods on both sides of the conducting periods of BLDC motors driven in the 120° conduction mode. The proposed sensorless control method integrates counter electromotive force in the non-conducting periods and adjusts the switching angle to control the values. Moreover, the proposed method can realize that sensorless strongly resistant to noise (by realizing sensorless) based on integrating counter electromotive force. By controlling the ratio of the integrated values of counter electromotive force can adjust switching periods and realize various controls such as field-weakening control. In addition, this paper tested the validity of the

proposed method by 4 kw-class 28-pole BLDC motors.

2. Materials and Methods

2.1. Sensorless Basic Topology Analysis

BLDC motors generate torque by sequentially applying voltage synchronized with the position of the rotor of stator armature windings using an inverter. In this case, BLDC motors are divided into BLDC motors with sinusoidal counter electromotive force and BLDC motors with trapezoidal counter electromotive force according to the shape of counter electromotive force. The former is used as a permanent magnet synchronous motor (PMSM). PMSM type can reduce torque ripple by maintaining input phase currents in the form of sinusoidal counter electromotive force and controlling the vector[5-9].

The latter, BLDC motors with trapezoidal counter electromotive force, generate stable torque by applying square wave currents to the fluttering region of counter electromotive force. The rotor position information is imperative to drive BLDC motors. To this end, location information is generally obtained using an encoder or a hall effect sensor.

However, sensorless driving without position sensors is frequently needed due to the field state or economic reasons. The simplest sensorless method is to drive in the 120° conduction mode by finding the zero-crossings of counter electromotive force at 60° intervals without applying voltage. Although there are various

sensorless driving methods for PMSM, it is complicated to realize them[10,11]. Therefore, there is an increased frequency of driving the 120° conduction mode for sensorless of PMSMs with sinusoidal counter electromotive force. Although this has the disadvantage that torque ripple greatly increases when applying square wave currents due to sinusoidal counter electromotive force, torque ripple matters little when it is operated at high speed. Figure 1 shows the counter electromotive force waveform of electric motors. Although counter electromotive force varies in proportion to the speed, the zero crossing of counter electromotive force always exists at a certain position angle. Therefore, in general, six absolute rotor positions are obtained by detecting counter electromotive force and zero crossing point with zero counter electromotive force. As shown in Figure 1, 30° phase difference exists at the time of switching with the zero crossing point. Thus, an algorithm is required to compensate for this. In order to obtain the zero crossing point of phase counter electromotive force, measurement is easy only when neutral wires of electric motors with Y-connection are exposed. However, neutral points of most electric motors are not drawn outside/ Therefore, it is necessary to set a virtual neutral point or reference source replacing the neutral point[12-15].

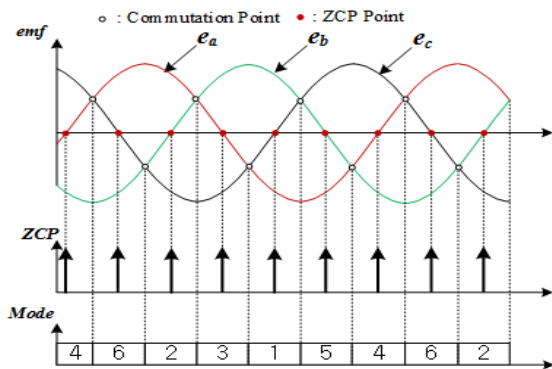


Figure 1: Back-EMF waveform of the motor ZCP

However, it is hard to use this method in the low-speed region with small counter electromotive force, and this method has the advantage of decreasing the position resolution at high speed because a phase lag filter is used to compensate for 30° phase difference at the time of switching with the zero crossing point. As shown in Figure 2 (b), virtual neutral points can be set by Y-connecting resistance. Although three high-frequency components appear in the trapezoidal counter electromotive force, they do not appear in the sinusoidal counter electromotive force. Thus, sensorless cannot be performed by three high-frequency components.

It is possible to obtain bipolar voltage based on the intermediate value of DC voltage. Thus, as shown in Figure 3, the counter electromotive force waveform in the non-conducting period symmetrically appears symmetrically when driving BLDC motors normally in the method for finding the zero crossings. In this case, the time when the zero crossing point becomes half of DC voltage in the lower limit of the measured voltage is the zero crossing point with zero counter electromotive force. Phase shift occurs in the measured counter electromotive force signals when all of three windings of an electric motor do not work ideally such as activation and excess load regulation. This makes it impossible to perform sensorless because abnormal currents flow in the windings. Moreover, this method has the disadvantage of having to generate voltage additionally to set the intermediate value of DC voltage as reference voltage.

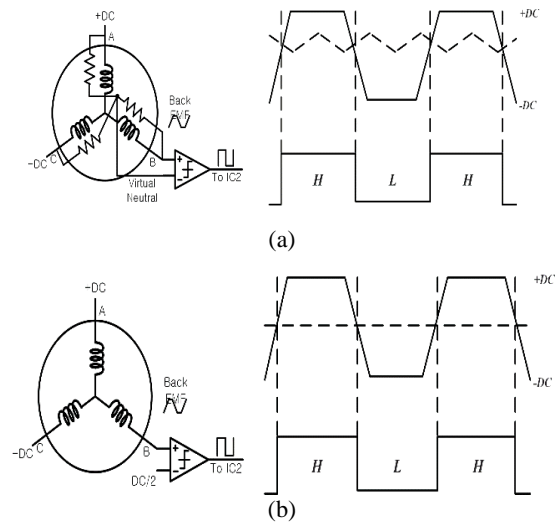


Figure 2: Detection method of back-EMF

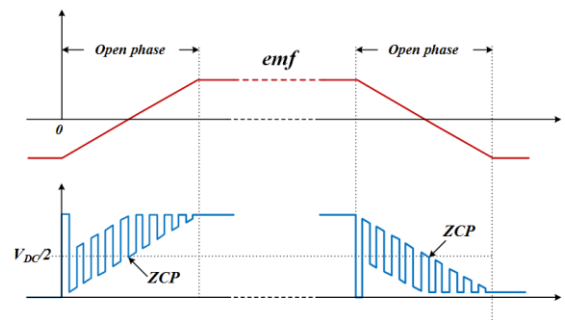


Figure 3: Non-conducting back-EMF and arm voltage waveforms

2.2. The Proposed Sensorless Method

As shown in Figure 4, this study adopted a method of detecting dark voltage of the inverter as terminal voltage of the electric motor with reference to the ground side of the inverter.

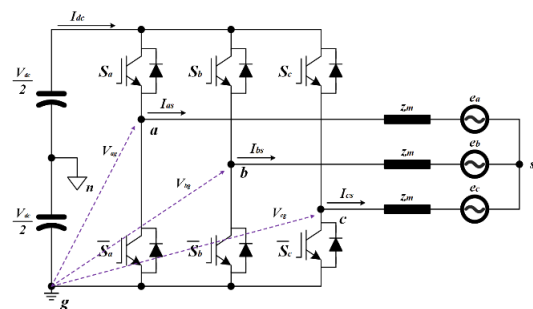
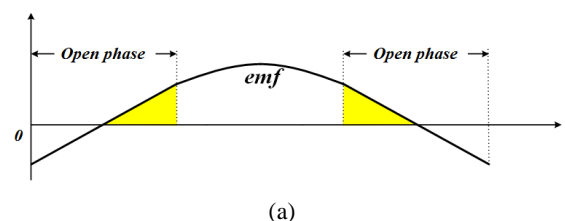


Figure 4: Sensorless configuration by arm voltage detection

Figure 4 shows the arm voltage waveform in the non-conducting period when driving PMSM with sinusoidal counter electromotive force. A voltage waveform is shown in Figure 5 (a) if arm voltage of the inverter is measured when BLDC motors with sinusoidal Back-emf normally drive. Floating periods appear at the anterior and posterior ends of this waveform, and the beginning and end of this section is the ZCP of counter electromotive force.



(a)

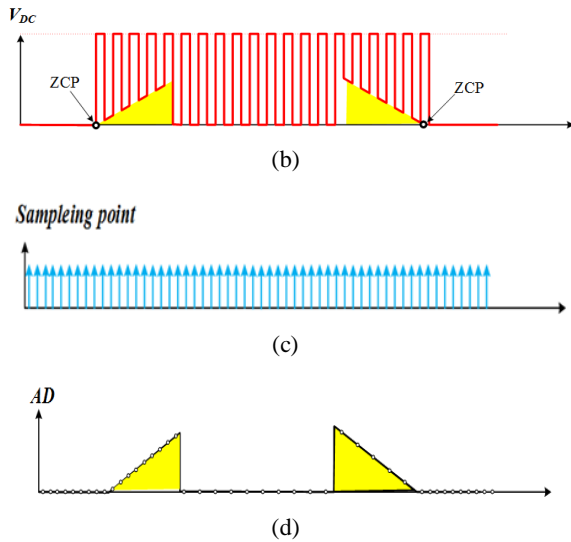


Figure 5: Back-EMF arm voltage, arm voltage measurement waveform

Arm voltage in the non-conducting period is overlapped with phase Back-emf by other arm PWM as shown in Figure 5(b). Therefore, in order to remove the effects of other arm PWM, sampling should be done in the intermediate portion of PWM as shown in Figure 5(c). In this case, Figure 5(d) shows the measured dark voltage. As shown in Figure 5(d), the measured phase counter electromotive force can appear symmetrically with reference to the maximum value of the actual counter electromotive force in Figure 5 (a). If phase shift occurs in the switching angle of BLDC motors, the measured counter electromotive force in Figure 5(d) cannot also have symmetry. Therefore, it will be able to perform stable sensorless if switching is performed in the inverter so that only the symmetry of the measured counter electromotive can be maintained. Although there are several methods for having symmetry, it is possible to consider the integral information on counter electromotive force to increase resistance to noise.

Figure 6 shows the measured dark voltage and the integral values in the non-excitation period when phase shift occurs in the switching angle in driving sensorless. As shown in Figure 6(a), the information on counter electromotive force appears in dark voltage only with positive counter electromotive force during the non-conducting excited period. This paper defines the integral value with increasing counter electromotive force in the non-conducting period as α and the integral value with decreasing counter electromotive force as β .

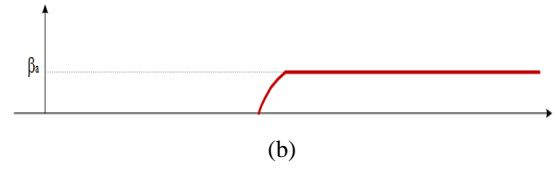
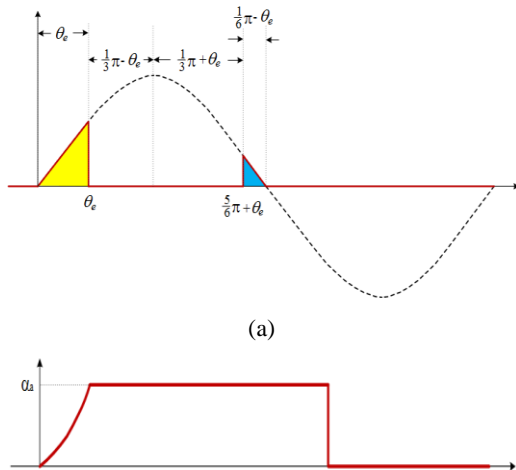


Figure 6: Back-emf, non-excitation phase back-emf integral value waveform

As shown in Figure 6(b), it will be able to calculate the switching angle to perform symmetrical switching if integral values in the non-excitation period are calculated. Integral values in the non-excitation period for sensorless are determined by the switching angle and phase counter electromotive force. Therefore, it is possible to calculate the switching angle using integral values of phase counter electromotive force if the information on phase counter electromotive force is obtained. If BLDC motors have a sinusoidal counter electromotive force waveform, it is possible to define as the following equation:

$$\begin{aligned} e_a &= K_e \omega_e \sin(\omega_e t) \\ e_b &= K_e \omega_e \sin\left(\omega_e t - \frac{2}{3}\pi\right) \\ e_c &= K_e \omega_e \sin\left(\omega_e t + \frac{2}{3}\pi\right) \end{aligned} \quad (1)$$

Thus, the integral values in the region with increasing back-emf in the non-exciting phase are as follows:

$$\alpha_a = K_e \int_0^{t_1} e_a(t) dt = K_e \int_0^{t_1} K_e \omega_e \sin(\omega_e t) dt \quad (2)$$

However, t_1 is the time corresponding to θ_e . Equation (2) is a time scaling function and works as a function that counter electromotive force changes with the motor electrical speed. When setting the integration axis as θ to simplify equation (2), the following equation is obtained:

$$\alpha_a = K_e \int_0^{\theta_e} K_e \sin(\theta) d\theta = K_e [1 - \cos(\theta_e)] \quad (3)$$

As shown in Equation (3), the integral function of counter electromotive force in the non-excitation period works independently from the motor electrical speed and is simply expressed as a function of switching angle (θ_e).

The integration values in the region where back-emf decreases on the non-excitation are as follows.

$$\beta_a = K_e \int_{\frac{5}{6}\pi + \theta_e}^{\pi} K_e \sin(\theta) d\theta = K_e [1 + \cos(\frac{5}{6}\pi + \theta_e)] \quad (4)$$

The condition that the BLDC is normally driven and is symmetrically switched based on the maximum point of back-emf is defined as Equation (5) when Equation (3) and Equation (4) have the same value.

$$\alpha_a = \beta_a \quad (5)$$

Therefore, given the angles of the symmetrically switched conditions for the sensorless stable operation of the BLDC, the equations (3), (4) and (5) to (6) are given.

$$-\cos(\theta_c) = \cos(\frac{5}{6}\pi + \theta_c) \quad (6)$$

Using the trigonometric function formula to obtain from Eq. (6), the following equation is obtained.

$$\sin(\frac{1}{2}\pi - \theta_c) = \sin(\frac{1}{6}\pi + \theta_c) \quad (7)$$

From the equation (7), it is as follows.

$$\theta_c = \frac{\pi}{6} \tag{8}$$

If the integral value in the region where the counter electromotive force increases on the non-excitation can be obtained from the equation (3), the switching angle is given by the following equation.

$$\theta_e = \arccos\left(\frac{K_e - \alpha_a}{K_e}\right) \tag{9}$$

If the integration value in the region where the counter electromotive force is reduced on the non-excitation can be obtained, the switching angle from Equation (4) is given by the following equation.

$$\theta_e = \arccos\left(\frac{\beta_a - K_e}{K_e}\right) - \frac{5}{6}\pi \tag{10}$$

From the equations, (9) and (10), the information about the switching angle can be obtained through the counter electromotive force integration before and after the switching operation of each arm.

With this information, the conversion error (θ_{error}) can be defined as follows.

$$\theta_{error} = \theta_c - \theta_e = \frac{1}{6}\pi - \theta_e \tag{11}$$

Therefore, the equation (11) can achieve stable sensorlessness by moving the defined switching angle error to the switching angle. Figure 7 shows the waveforms of integral values of three-phase and non-excitation back-emf.

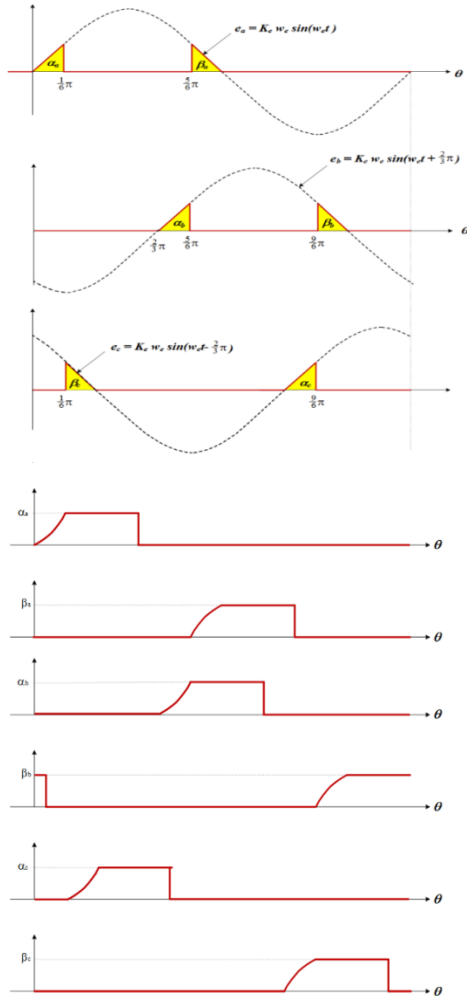


Figure 7: 3-phase back-emf and non-excitation counter electromotive force integral value

3. Experimental Results

3.1. System Configuration

Table 1 shows the specifications of the motor under test.

Table 1: Under test motor specification

Specification	
RPM/V(KV)	120 [RPM/V]
Weight w/o Wires	1000 [g]
Diameter	89 [mm]
Length	64.0 [mm]
Slots, Poles	24,28
Idle Current(Io) @10V	1.4 [A]
Resistance	36 m[\Omega]
Inductance	30 [\mu H]
Nominal Voltage	30-51 [V]
Cruising power[30mins]	2730 [W]
Bursts Current[30s]	112 [A]
Peak power(30s)	5 k[W]

Figure 8 shows the overall system block diagram of the proposed rotor position estimation algorithm. Open-loop control to activate BLDC motors determines the application switch in the inverter by the vector generator by calculating the position using an integrator when speed is generated. When the electric motor speed reaches the region capable of stably detecting counter electromotive force, voltage values are selectively integrated according to the switching mode by sampling AD to detect Vag, Vbg, and Vcg in the intermediate portion of PWM low region to reduce the effects of other dark PWM. The integral values of counter electromotive force are used as information to generate switching vector by calculating switching errors using the method proposed in the preceding section and correcting position estimation errors. The speed information on electric motors is obtained by values counting the time of switching vector. When switching algorithm is stabilized, vector voltage is controlled using current and voltage controllers by the information on command and estimated speed. In addition, current limits were set by speed functions for stabilization.

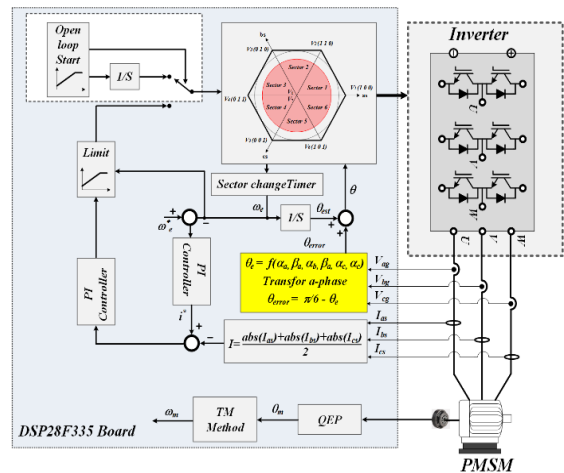


Figure 8: System control block diagram

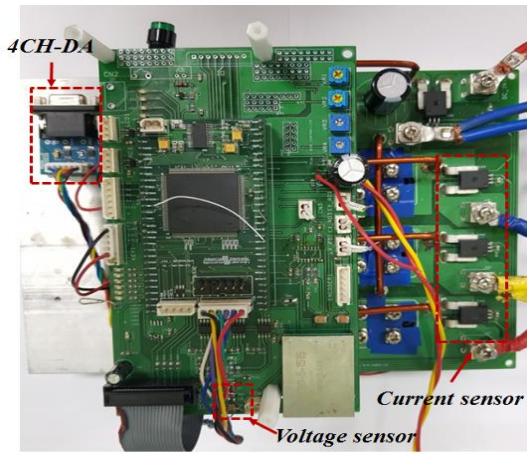
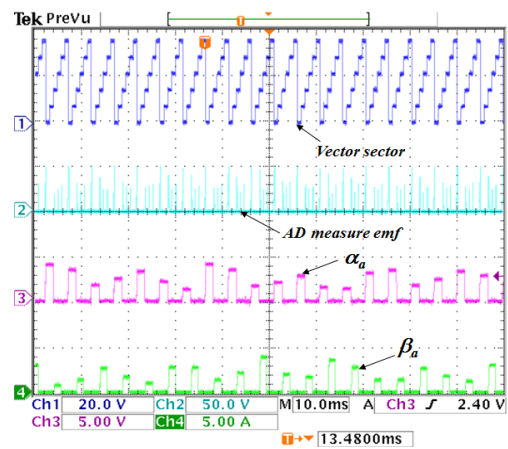


Figure 9: Power conversion device and BLDC controller

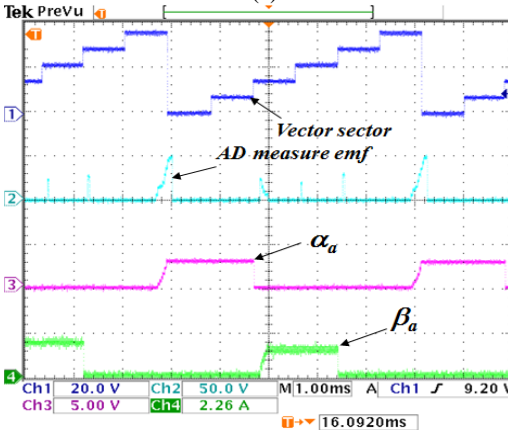
The power converter consists of a three-phase PWM inverter, sensing, and control board. As shown in Figure 9, BLDC motors are controlled with 120° conduction angle. 200V switching element and 140A-class MOSFET were used for the three-phase PWM inverter. Allegro ACS758 was used as a sensor for current measurement. The main controller was self-designed exclusively for controlling three-phase electric motors using Texas Instruments DSP (TMS28335). In addition, 4-channel 16 bit D/A was used to validate the inner and output variables.

3.2. Experiment Result

Figure 10 shows the integrated waveform of counter electromotive force in the measured dark voltage and non-excited phase sampled in the intermediate portion of the return vector and PWM.



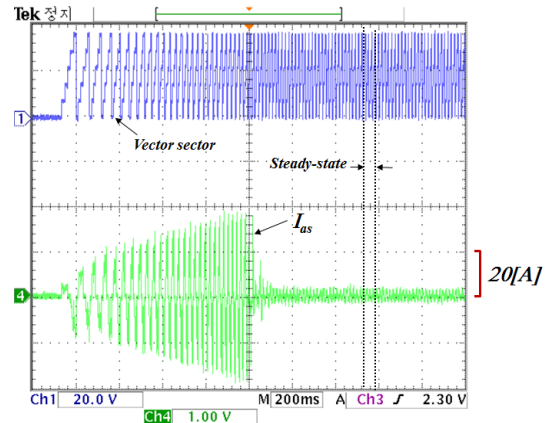
(a)



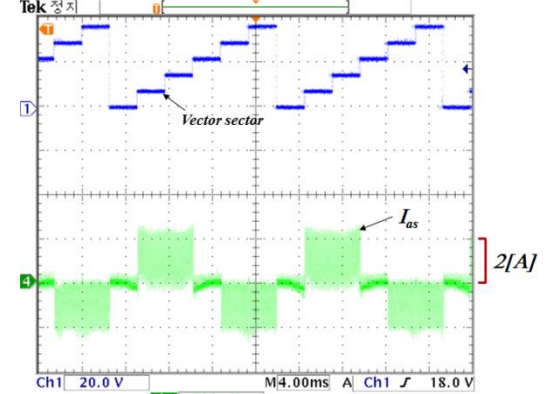
(b)

Figure 10: Non-excitation phase back-emf integral characteristic waveform

As shown in Figure 10, good sensorless is performed because switching is conducted symmetrically with phase counter electromotive force and the integral value (α_a) with increasing counter electromotive force is evenly maintained with the integral value (β_a) with decreasing counter electromotive force.



(a) Starting Characteristic

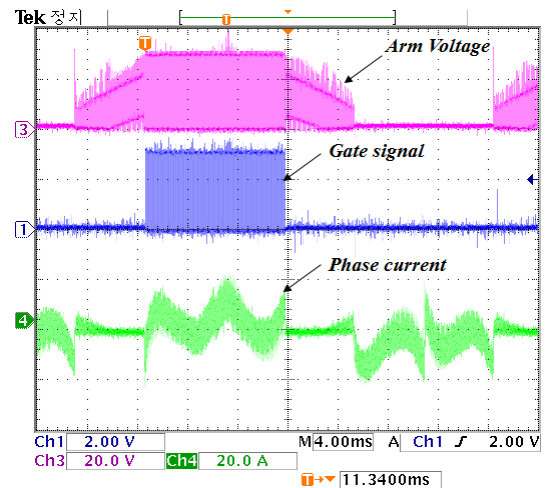


(b) Steady state after startup

Figure 11: Startup characteristic waveform

Figure 11 shows the estimate position angles and phase currents to check the starting characteristics.

As shown in Figure 10 (a), the starting current increases up to approximately 40 [A], and phase switching is performed well after open-loop control finishes at approximately 50 [Hz]. It smoothly drives in the normal state at approximately 210 [rpm] after the start-up.



(a)

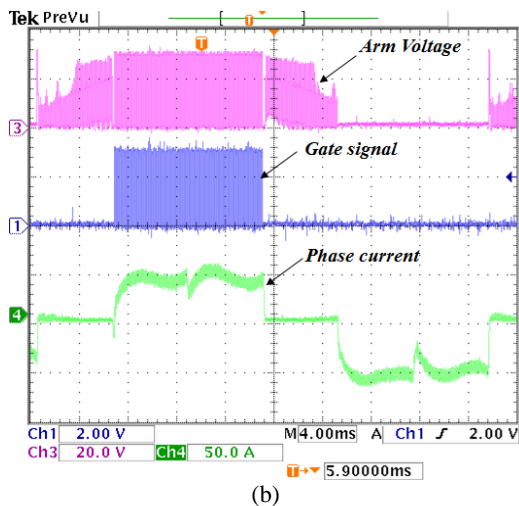


Figure 12: Phase current waveform according to load

Figure 12 shows the waveform to analyze the current waveform characteristics according to load in BLDC motors with sinusoidal counter electromotive force. Although phase current ripple was large, the effects decrease under heavy load.

As shown in Figure 13, driving is performed smoothly even when changing load through the waveforms of excitation voltage and phase currents when rapidly changing load periodically at 4,000[W]/400[W].

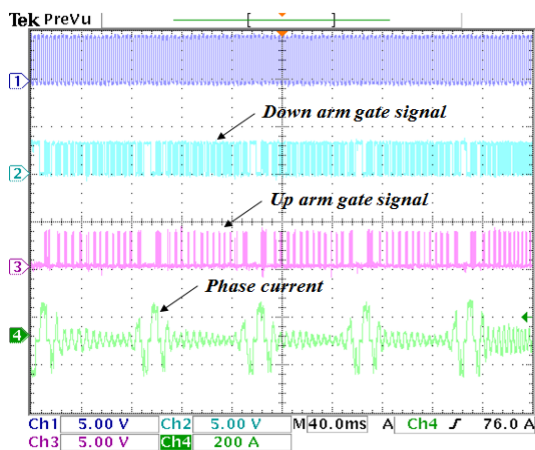


Figure 13: Excitation voltage and phase current waveform during sudden change in load

4. Conclusion

There is a compelling need for densificated high-efficiency BLDC system satisfying various demands for plants as the electric motor fields have been widely used. In particular, with the development of the electric motor industry, various capacity BLDC motors have been actively produced. Furthermore, studies on sensorless control methods have attracted attention because of the production of multipole BLDC motors.

In this paper proposed a new sensorless control method for switching angles by counter electromotive force in the non-conducting periods on both sides of the conducting periods of BLDC motors driven in the 120° conduction mode. The proposed method can realize that sensorless strongly resistant to noise based on integrating counter electromotive force. In addition, by controlling the ratio of the integrated values of counter electromotive force can adjust switching periods and realize various controls such as field-weakening control. As a result of the test, it was confirmed that sensorless control was realized against even severe load variation.

References

- [1] T.H. Kim, H.W. Lee and M. Ehsani, "Advanced sensorless drive technique for multiphase BLDC Motors", *IEEE IECON* vol.1 pp. 926-931
- [2] J. C. Moreira, (1996). "Indirect Sensing for Rotor Flux Position of Permanent Magnet AC Motors Operating Over a Wide Speed Range," *IEEE Trans. Ind. Appl.*, vol. 32, no. 6, pp. 1392-1401.
- [3] H. R. Andersen and J. K. Pedersen, (1997). "Sensorless ELBERFELD Control of Brushless DC Motors for Energy-Optimized Variable-Speed Household Refrigerators," *EPE Conf. Rec.*, vol. 1, pp. 314-318.
- [4] Hyeong-Gee Yee, Chang-Seok Hong, Ji-Yoon Yoo, Hyeon-Gil Jang, Yeong-Don Bae and Yoon-Seo Park, (1997). "Sensorless Drive for Interior Permanent Magnet Brushless DC Motors," *Electric Machines and Drives Conf. IEEE International*. pp 18-21.
- [5] P. Pillay and R. Krishnan, (1991). "Application Characteristics of Permanent Magnet Synchronous and Brushless dc Motors for Servo Drives", *IEEE Trans. on Ind. Appl.*, vol. 27, no. 5, pp. 986-996.
- [6] Paul E. Scheiing, et al., (2007). "United States Industrial Motor-Driven Systems Market Assessment: Charting a Roadmap to Energy Saving for Industry," *U.S. Department of Energy*.
- [7] S. J. Chapman, (1999). *Electric Machinery Fundamentals*, 3rd ed., McGrawHill.
- [8] G.R. Slemmon and A. Straughen, (1980). *Electric Machines*, 2nd ed., Addison-Wesley.
- [9] Werner Leonhard, (1996) *Control of Electrical Driver*, 2nd ed., Springer.
- [10] T.M. Jahns and W. L. Soong, (1996). "Pulsating Torque minimization technique for permanent magnet ac motor drives – A review," *IEEE Trans. On Industrial Electronics*, vol. 43 pp. 321~330, Apr.
- [11] B. K. Bose, (1996). *Power Electronics and Variable Frequency Drives-Technology and Application*, *IEEE Press*.
- [12] K. Iizuka, et al., (1985). "Microcomputer control for sensorless brushless motor," *IEEE Trans. On Industry Applications* vol. 27, pp595~601
- [13] J. Moreira, (1996). "Indirect sensing for rotor flux position of permanent magnet ac motor operating in a wide speed range," *IEEE Trans. On Industry Applications*, vol. 32, pp. 401~407.
- [14] H. -C. Chen T.-Y. Tsai C. -K. Huang, (2009) "Low-speed performance comparisons of back-EMF detection circuits with position-dependent load torque," *IET Electr. Power Appl.*, vol. 3, Iss 2, pp. 160~169.
- [15] T. KIM, H-W. Lee and M. Ehsani, (2007). "Position sensorless brushless DC motor/generator driver : review and future trends," *IET Electr. Power, Appl.*, vol. 1, Iss. 4, pp. 557~564.